Hindawi
International Journal of Aerospace Engineering
Volume 2022, Article ID 9684007, 22 pages
https://doi.org/10.1155/2022/9684007

Research Article

Nonuniform Clearance Effects on Pressure Distribution and Leakage Flow in the Straight-through Labyrinth Seals

Yu Shi,[1] Shuiting Ding,[1,2] Tian Qiu,[2] Peng Liu,[2] and Chuankai Liu[2]

[1]*School of Energy and Power Engineering, Beihang University, Beijing 100191, China*
[2]*Research Institute of Aero-Engine, Beihang University, Beijing 100191, China*

Correspondence should be addressed to Peng Liu; liupeng91@buaa.edu.cn

Received 17 June 2022; Revised 17 November 2022; Accepted 6 December 2022; Published 20 December 2022

Academic Editor: Hongbing Ding

Straight-through labyrinth seal is a simple and reliable noncontact seal structure widely used in aeroengines. During the actual operation of aeroengines, the labyrinth seal clearance might experience a nonuniform variation in the flow direction due to asymmetric structure and uneven temperature. In order to characterize the degree of nonuniformity, the nonuniformity coefficient is defined in current paper. The effect of nonuniform causes (rotor deformation or stator deformation), nonuniform type (convergent clearance or divergent clearance), and nonuniformity coefficient (nonuniformity degree) is carefully studied by numerical simulation. Comparative analysis has shown that there is no obvious difference in flow coefficient (less than 0.8% in current studies) between two nonuniform causes. As for nonuniform type, the nonuniformity impact of divergent type on the flow coefficient is more significant than that of convergent type, as a result of stronger axial inertia. Pressure distributions of teeth cavities indicate that the total pressure drop of the divergent type is more obvious than that of the convergent type when the pressure ratio is the same. With the same dimensionless minimum tip clearance, clearance nonuniformity would result in the increase of leakage flow of the straight-through labyrinth, particularly for the condition with small pressure ratio, large circumferential Mach number, and small dimensionless minimum tip clearance. When the nonuniformity coefficient is within the range of -0.1 to 0.1, the variation curves of nonuniformity impact factor versus the nonuniformity coefficient almost coincide (the maximum deviation is no more than 1.2%) under different operation conditions (Reynolds number, pressure ratio, circumferential Mach number, and dimensionless minimum tip clearance). Current work proves it that the effect of seal clearance nonuniformity on the leakage flow requires special attention for the refined design of aeroengines.

1. Introduction

The secondary air system (SAS) plays an important support role to ensure the safe and efficient operation of aeroengines. [1] Increasing demands for high performance, energy-saving, and safety levels for aeroengines are attracting more interest in the accurate analysis and refined design of the secondary air system. Labyrinth, as an important noncontact rotor-stator sealing device, has been widely used in the secondary air system of aeroengines due to its simple structure and high reliability. Labyrinth seal performs as a metering device to control internal airflow, thereby affecting some safety-related functions of SAS (prevention of hot gas ingestion into the turbine disk cavities, turbine blade cooling, and axial bearing loading control). Therefore, the labyrinth sealing flow should be analyzed meticulously for the sake of safety.

A large number of scholars have made detailed studies on the factors affecting the sealing flow of labyrinths, including rotational speed [2–4], Reynolds number [5], pressure ratio [6], and geometric parameters [5–9]. The structure of labyrinth is complex, and there are many geometric parameters that affect the sealing flow, such as radius, sealing clearance, tooth tip width, tooth height, tooth pitch, stage number, and inclination angle. Zhao and Wang [10] carried out shape optimization of a straight labyrinth seal to reduce gas leakage and pointed out that the sealing clearance was one of the important optimized parameters. Other researches also revealed that the influence of labyrinth sealing clearance on sealing flow is particularly significant [3,

5, 6, 11–14]. Nayak [3] claimed that the effects of rotation on leakage characteristics of straight-through labyrinths were not exactly the same under different sealing clearance. Li et al. [4] investigated the effects of pressure ratio and rotational speed on leakage flow and cavity pressure in the staggered labyrinth seal. Hu et al. [5] illustrated that flow resistant characteristics of straight-through labyrinths were related to the ratio of equivalent diameter (double sealing clearance) to seal length. Wu and Andrés [6] found cavity pressure reduced, but seal leakage rose with the increase of sealing clearance. Wu and Andrés [11] also investigated the effect of sealing clearance on wall friction factors, relating to sealing flow in labyrinth seals. Yan et al. [12] studied the effect of sealing clearance change caused by teeth bending and mushrooming damages on leakage performance of straight-through labyrinth seals. Andrés et al. [13] compared the sealing leakage and tooth cavity pressure distribution with or without swirl brakes under three different sealing clearances. Lee et al. [14] carried out flow visualization measurement within the labyrinth seal by Schlieren method, investigating the influence of dimensionless sealing clearance on the leakage flow. They also pointed out that the leakage characteristics of stepped and straight-through seals showed different trends. As summarized, sealing clearance is recognized as one of the most important factors affecting sealing flow in labyrinth seals. However, much of the research up to now has been carried out under a fixed clearance.

In the actual operations of aeroengines, the sealing clearance of labyrinth would be variable due to the deformation of components caused by mechanical loads and thermal loads. Considering the sealing clearance difference, Li et al. [15] measured leakage coefficients of labyrinth seal in the cold and hot states and compared them with floating ring seal. Kong et al. [16, 17] also paid attention to the variation of labyrinth clearance due to centrifugal deformation when investigating the sealing performance of rotating labyrinth. The labyrinth clearance was measured to include the effects of labyrinth clearance variation on leakage flow. Eastwood et al. [18] built an advanced multiconfiguration stator well cooling test facility and carried out displacement measurements for sealing clearance. The hot running seal clearance grew up by approximately 30% of cold build clearance. Ganine et al. [19] used solid finite element model coupled with one-dimensional flow network to predict radial clearances evolution of the 14 labyrinth seals in a square cycle. From their simulation results, the widest range of radial clearance variation was about from 40% to 180% of cold built clearance.

However, the sealing clearance profile of the deformed labyrinth may not always keep uniform during the engine operation process. Recent evidence has shown that thermal expansion may also make sealing clearance nonuniform along the flow direction due to the uneven temperature distribution [20]. Sun et al. [21] found that convergent and divergent clearance profiles have different effects on leakage flow when the nonuniformity degree is the same. Shi et al. [22] discussed the effects of nonuniform clearance on windage heating and swirl development under different Reynolds numbers, pressure ratios, circumferential Mach numbers, and dimensionless minimum clearances. Up to now, the nonuniform clearance effects on pressure distribution and leakage flow in the straight-through labyrinth seal is still lack of systematic and in-depth research. The leakage flow characteristics of the labyrinth with a nonuniform clearance are not clear, leading to an inaccurate flow prediction of SAS in the operation of aeroengines. In current studies, the straight-through labyrinths are taken as the investigation objective, and the nonuniformity coefficient is proposed to characterize the degree of the sealing clearance nonuniformity. The influences of the sealing clearance nonuniformity (nonuniform causes, nonuniform type, and nonuniformity coefficient) on the pressure distribution and the leakage flow are discussed in detail. This investigation reveals new understanding into the labyrinth sealing performance, contributing to the performance assessment and safety design of the aerothermomechanical system, including aeroengines.

2. Methodology

2.1. Description of Nonuniform Sealing Clearance

2.1.1. Geometric Configuration. A straight-through labyrinth is regarded as the research objective of this investigation, which consists of four stages of labyrinth teeth, as shown in Figure 1. The reasons of nonuniform deformation of sealing clearance usually include asymmetric structure and uneven temperature, resulting in the monotonic profile of the labyrinth tip clearance. The labyrinth clearance becomes larger or smaller gradually along the flow direction as shown in Figure 2. Generally, the labyrinth seal has a pretty tiny axial dimension, structured no more than tens of millimeters. In such a limited space, the tip clearances of different stages caused by the nonuniform deformation can be simplified to be linear distribution according to the previous investigation [21–23]. Therefore, in this work, the assumption of the linear clearance profile is also adopted, and the nonuniformity coefficient u is employed to depict the nonuniformity of the labyrinth seal clearance as defined in the authors' previous investigation [22]. The absolute value of the nonuniformity coefficient $|u|$ can symbolize the nonuniformity degree of the labyrinth seal clearance, which is defined as the ratio of the maximum tip clearance deviation to twice of the average sealing clearance.

$$|u| = \frac{c_{\max} - c_{\min}}{2c_{\text{av}}}. \tag{1}$$

$c_{\max}$ is the maximum tip clearance, $c_{\min}$ is the minimum tip clearance, and c_{av} is the average tip clearance.

As for a labyrinth with four stages of teeth, Equations (2) and (3) provide the calculation method of the average labyrinth tip clearance and the nonuniformity coefficient.

$$c_{\text{av}} = \frac{1}{4}\sum_{i=1}^{4} c_i, \tag{2}$$

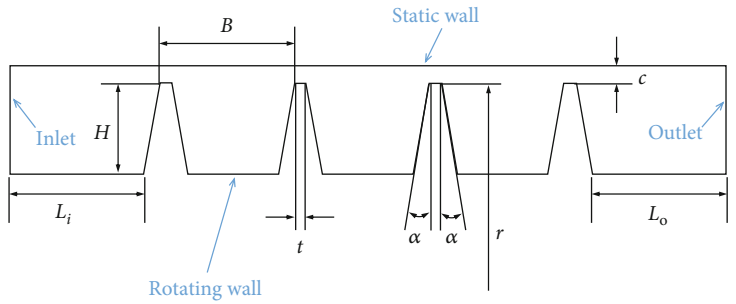

Figure 1: Geometric model.

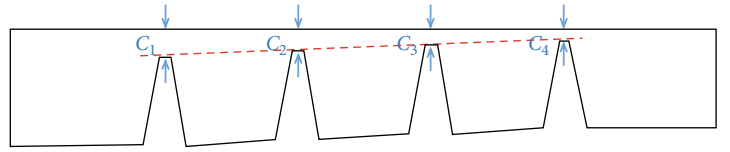

Convergent seal clearance ($C_1 > C_2 > C_3 > C_4$)

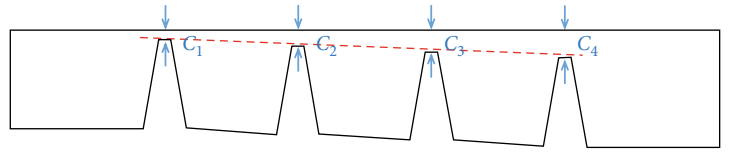

Divergent seal clearance ($C_1 < C_2 < C_3 < C_4$)

Figure 2: Nonuniform seal clearance.

$$u = \frac{c_1 - c_4}{2c_{av}}. \tag{3}$$

c_i is the tip clearance of the i^{th} stage. $|u| = 0$ implies a uniform sealing clearance, and $|u| = 1$ implies a zero minimum labyrinth tip clearance, meaning a situation of rub-impact.

The convergent type of sealing clearance is characterized by $u > 0$, while the divergent type of sealing clearance is characterized by $u < 0$. The critical safety-limit parameter for the seal device is the minimum tip clearance. Consequently, the minimum clearance, replacing the mean clearance, together with the nonuniformity coefficient is regarded as the key geometric parameter for clearance nonuniformity description. In this investigation, the minimum tip clearance range is $0.2\,\text{mm} \le c_{min} \le 0.6\,\text{mm}$, and the nonuniformity coefficient range is $-0.5 \le u \le 0.5$. Table 1 includes other detailed geometric dimensions. The meaning of each parameter has been explained in Figure 1.

2.1.2. Dimensionless Parameters. In the labyrinth seal, after the airflow is accelerated by the throttling of the former tip clearance, the kinetic energy of the fluid cannot be completely dissipated into thermal energy in the following cavity. Because of the inertia, part of the kinetic energy is directly transported from the upstream throttle to the downstream throttle. The kinetic energy carry-over effect will weaken the sealing ability. The axial Mach number M_A is an important parameter to describe the axial inertia in the labyrinth seal, which is defined as

Table 1: Geometric parameters.

Parameter	Value
α	10°
B	6 mm
H	4 mm
L_i	6 mm
L_o	6 mm
r	254 mm
t	0.5 mm

$$M_A = \frac{V_A}{a}. \tag{4}$$

V_A is the axial velocity of airflow, and a is the local sound speed.

In this study, the pressure coefficient ψ is adopted to characterize the dimensionless total pressure [4, 24]. The definition is shown in

$$\psi = \frac{p_t - p_{s,out}}{p_{t,in} - p_{s,out}}. \tag{5}$$

p_t is total pressure in a tooth cavity, $p_{t,in}$ is total pressure of seal inlet, and $p_{s,out}$ is static pressure of seal outlet.

Total pressure drop is an important characterization of the labyrinth seal. For the whole labyrinth seal, the pressure load of labyrinth seal $\Delta\psi_{\text{seal}}$ is defined as the pressure coefficient difference between the inlet and the outlet, as shown in Equation (6). For a single stage of the labyrinth tooth, the pressure load of labyrinth tooth $\Delta\psi_i$ is defined as the pressure coefficient difference between the front and rear tooth cavity, regarded as the contribution to the total pressure drop, shown in Equation (7).

$$\Delta\psi_{\text{seal}} = \psi_{\text{inlet}} - \psi_{\text{outlet}}, \tag{6}$$

$$\Delta\psi_i = \psi_i - \psi_{i+1}. \tag{7}$$

ψ_{inlet} and ψ_{outlet} are the pressure coefficient of labyrinth seal inlet and outlet, respectively. ψ_i is the pressure coefficient in the i^{th} teeth cavity.

As one of most important characteristic quantity, the flow coefficient [4, 24, 25] is introduced to characterize the dimensionless mass flow rate. The definition is shown in

$$\varphi = \frac{\dot{m}(RT_{\text{t,in}})^{1/2}}{Ap_{\text{t,in}}}. \tag{8}$$

$\dot{m}$ is leakage mass flow rate, $T_{t,\text{in}}$ is inlet total temperature of seal inlet, R is gas constant, and A is the cross-section area of the labyrinth tip clearance. For labyrinths with nonuniform tip clearances, cross-section area of the labyrinth minimum tip clearance A_{min} is used in Equation (8) instead of A.

Denecke et al. [26] made a dimensional analysis on the leakage flow of rotating labyrinth seal and simplified the parameters affecting flow characteristics according to the results of numerical simulation. Denecke et al. thought that flow characteristics were in connection with axial Reynolds number, effective pressure ratio, circumferential Mach number, geometric parameters, inlet preswirl ratio, specific heat ratio, and Prandtl number. In this study, the inlet preswirl is not the focus of the nonuniform clearance effect, so the air enters the sealing structure along the axial direction in the subsequent numerical simulation, in that situation where the ratio of inlet total pressure to outlet static pressure $\pi = p_{t,\text{in}}/p_{s,\text{out}}$ is equivalent to the effective pressure ratio [26]. Specific heat ratio and Prandtl number are considered as temperature-independent since the air would get little temperature increase within the sealing device. As for the geometric parameters, only the seal clearance, including the minimum tip clearance and the nonuniformity coefficient, is investigated to get insight into the influence of the nonuniform clearance. To improve the universality of research results, the minimum tip clearance is normalized by the labyrinth pitch. Nonuniformity coefficient u and dimensionless minimum tip clearance $C = c_{\text{min}}/B$ are employed jointly to depict the sealing clearance. Consequently, flow coefficient and pressure coefficient of the labyrinth seal can be expressed as

$$\varphi = f(\pi, \text{Re}, M_U, C, u). \tag{9}$$

Definitions of Reynolds number Re and circumferential Mach number M_U are shown in Equations (10) and (11), respectively.

$$\text{Re} = \frac{2\rho V c_{\text{min}}}{\mu} = \frac{\dot{m}}{\mu \Pi r}, \tag{10}$$

$$M_U = \frac{\Omega r}{a}. \tag{11}$$

ρ, μ, and V are the density, the dynamic viscosity, and the velocity of the labyrinth seal inlet, respectively. r is the radius of the labyrinth teeth tip, Π is circumference ratio, Ω is angular velocity of labyrinth rotor, and a is local sound speed.

In this investigation, the effect of clearance nonuniformity on the leakage flow is focused on, so the nonuniformity impact factor E is defined to describe the influence of nonuniformity degree on the flow coefficient, shown as

$$E = \frac{\varphi_u}{\varphi_0}. \tag{12}$$

φ_u is the flow coefficient of the nonuniform clearance labyrinth ($u \neq 0$), while φ_0 is the flow coefficient of the uniform clearance labyrinth ($u = 0$) with the same minimum tip clearance.

2.2. Numerical Simulation Method

2.2.1. Numerical Model. The commercial solver ANSYS CFX is adopted for the numerical simulation. Due to the rotational periodical characteristics of geometry and flow structure, a periodic symmetry model of three-dimensional labyrinth seal flow is adopted in the numerical simulation, in which the hexahedral structured grids are shown in Figure 3. The numerical setup is depicted in Table 2. Steady state analysis is conducted to simulate the seal flow. The working medium in the fluid domain is compressible ideal air. The heat transfer option is selected as the total energy model in the ANSYS CFX preprocessor. The Shear Stress Transport (SST) turbulent model is used to close the Reynolds stress terms. According to the recommendation of SST turbulent model, the maximum wall y^+ is near 1, so the grids around the labyrinth rotor and stator are refined locally to satisfy the computation requirement. The convection terms discretization and the turbulence terms discretization are all carried out by high resolution scheme.

Table 2 also includes the boundary conditions. The labyrinth rotor and stator are assigned as adiabatic wall. The rotating speed of the labyrinth rotor is within the range of $3000\ \text{rpm} \leq \Omega \leq 12000\ \text{rpm}$ corresponding to the circumferential Mach number scope of $0.23 \leq M_U \leq 0.92$. The total temperature of 300 K and the turbulence intensity of 5% are set for the labyrinth inlet. As for the pressure boundaries, the total pressure is assigned to the inlet, and the back pressure (static pressure) is assigned to the outlet. Moreover, a negative feedback method [22] is adopted in order to accurately control the pressure ratio independently with the Reynolds number. The pressure ratio scope of $1.03 \leq \pi \leq 4$

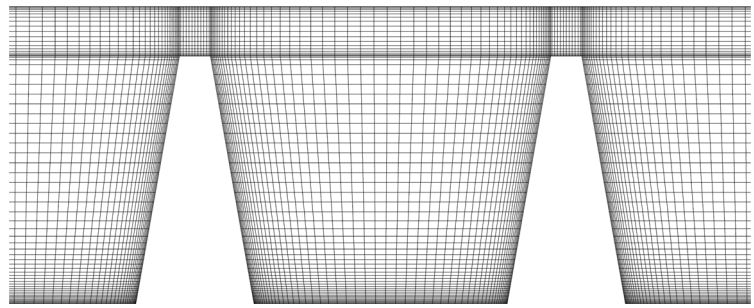

Figure 3: Mesh.

and the Reynolds number scope of $500 \le \mathrm{Re} \le 25000$ can cover the most common operating state of aeroengine labyrinth seals. The influence of the sealing clearance is the core of this study. Typical labyrinth clearance profiles in the aeroengine are usually within the dimensionless minimum tip clearance scope of $0.033 \le C \le 0.100$ (corresponding to 0.2 mm $\le c_{\min} \le$ 0.6 mm) and the clearance nonuniformity coefficient scope of $-0.5 \le u \le 0.5$.

2.2.2. Validation of Simulation Results. A grid sensitivity analysis has also been performed to define the mesh size. Three sets of grids with different element numbers are established. Element numbers of coarse, medium, and refined meshes are 21.2 thousand, 44.6 thousand, and 91.4 thousand, respectively. The calculations are carried out under the condition of uniform sealing clearance, that is $u = 0$. The grid independence validation is carried out under the uniform sealing clearance situation. The dimensionless tip clearance C is 0.067 (corresponding to a sealing clearance of 0.4 mm). In the verification case, the pressure ratio varies from 1.03 to 4, and the circumferential Mach number is 10000 (corresponding to a rotating speed of 3000 rpm). The computational convergence is accepted when the residuals of continuity equation, momentum equation, and energy equation converge to the order of 2×10^{-6}.The results of flow coefficients are depicted in Figure 4. The results illustrate that the maximum flow coefficient deviation of different grids is no more than 1.5%. Especially, less than 0.2% difference is observed between refine grid and medium grid. The flow coefficient results of medium grids can be convinced as independent from the mesh size. Considering the compromise between simulation accuracy and calculation cost, the medium grids are selected for subsequent calculation and analysis.

In order to validate the accuracy of the numerical model in current investigation, leakage mass flow rate and windage heating power test data of Millward and Edwards [27] are compared with the simulation results. The experimental investigation was carried out on the Rolls-Royce Internal Air Systems Research facility, installed on the Hucknall Thermal Site. The test configuration was a straight-through labyrinth seal with five stages of teeth under the rotational speed of 13000 rpm. Two groups of experiment data (run 4 and 5) are extracted for numerical simulation method validation. The sealing clearances of both run 4 and 5 were uniform. Specifically, the running sealing clearances of run 4 were 0.75 mm, and that of run 5 was 0.25 mm as described

Table 2: Numerical method and boundary conditions.

Analysis type	Steady state
Fluid	Air ideal gas
Heat transfer	Total energy
Turbulence model	SST
Discretization scheme	High resolution
Grid	Periodic hexahedral elements
Wall	Adiabatic
Inlet total temperature	300 K
Inlet turbulence intensity	5%
Pressure ratio	$1.03 \le \pi \le 4$
Reynolds number	$500 \le \mathrm{Re} \le 25000$
Circumferential Mach number	$0.23 \le M_U \le 0.92$
Dimensionless minimum tip clearance	$0.033 \le C \le 0.100$
Nonuniformity coefficient	$-0.5 \le u \le 0.5$

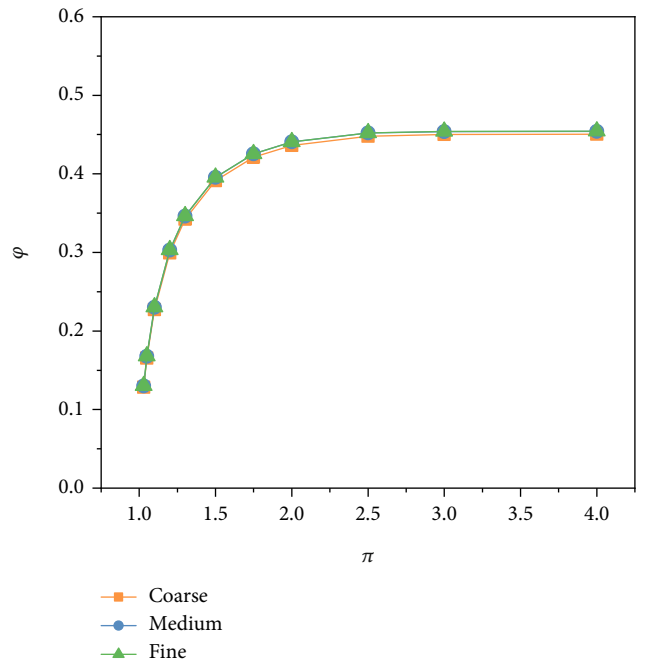

Figure 4: Grid sensitivity validation.

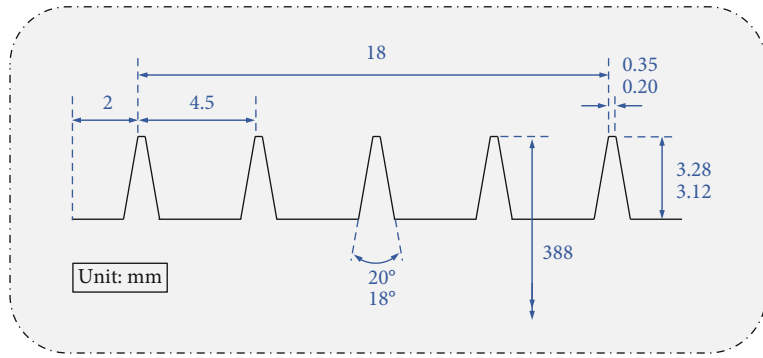

Figure 5: Test configuration [27].

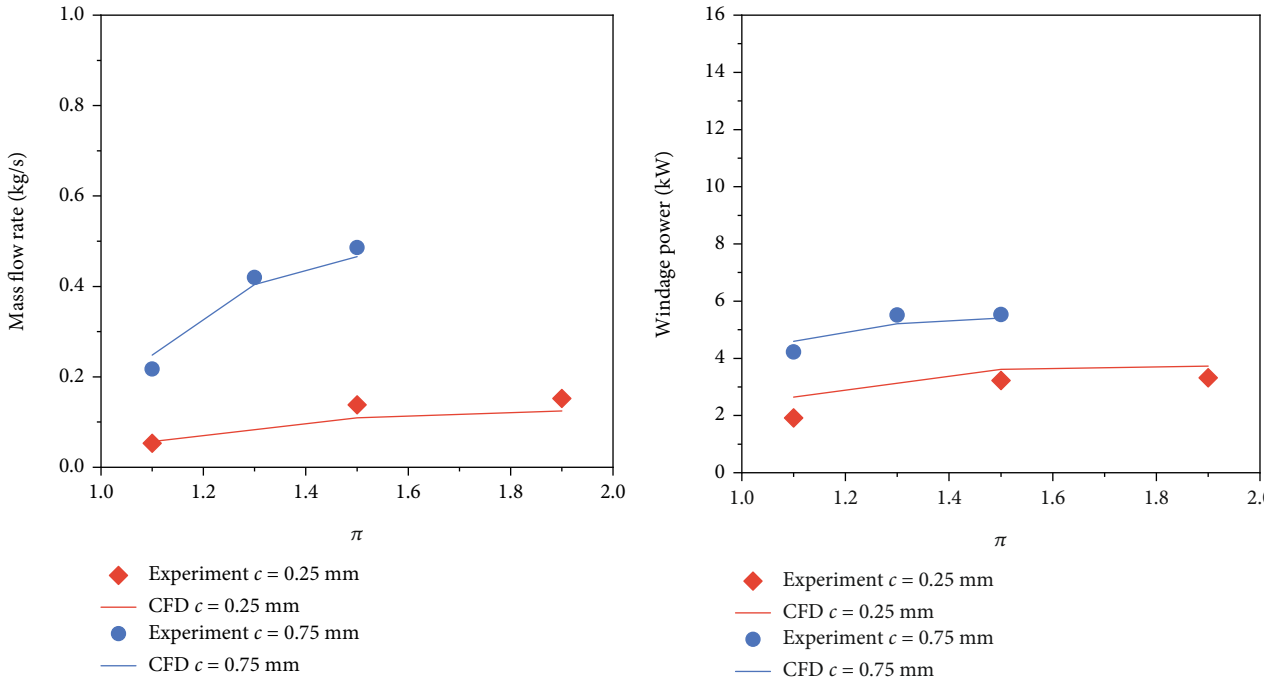

(a) Seal leakage comparison

(b) Windage power comparison

Figure 6: Validation of numerical simulation results [27].

in literature [27]. Other geometric parameters of the experiment configuration are claimed in Figure 5. The mass flow rate and the temperature rise of the air passing through the seal were measured in the experimental work. Further, the windage heating power of the labyrinth seal was derived from the enthalpy rise of the leakage flow. The validation range of pressure ratio is from 1.1 to 1.9. The comparison between the numerical simulation results and experimental data is displayed in Figure 6. The two data are in good agreement, proving that the numerical simulation model has sufficient calculation accuracy. In conclusion, the numerical simulation method in this work is applicable for the leakage flow in the straight-through labyrinth seal.

3. Results and Analysis

3.1. Effects of Nonuniformity Cause. During the operation process of aeroengines, both the rotor and the stator of labyrinth seal can experience different extents of radial deformations. The nonuniformity of labyrinth sealing clearance is the combined results of both deformations. Taking the convergent type clearance as an example, Figure 7 shows the structural diagram of nonuniform sealing clearances with equal stator radius (ESR) and equal rotor radius (ERR). The clearance nonuniformity of ESR is considered to be caused by rotor deformation, while the clearance nonuniformity of ERR is considered to be caused by stator deformation. The flow structure, pressure distribution, and leakage flow in cases of ESR and ERR are compared to clarify the effect of the nonuniformity cause.

Figure 8 compares the flow structure between the ESR and the ERR. The results indicate that the flow structure in the straight-through labyrinth seal is not sensitive to the nonuniformity cause. In cases of $u = -0.1$, $u = -0.2$, and $u = -0.3$, there is not obvious difference for the streamline distributions between the ESR and the ERR. As for the pressure

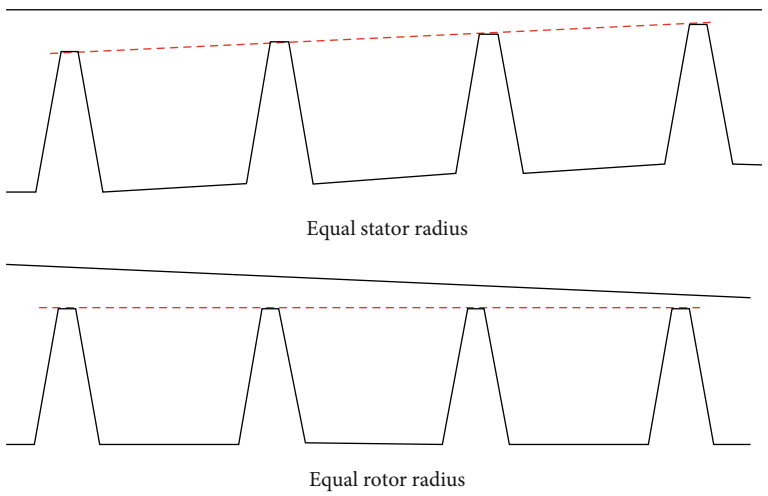

Figure 7: Convergent type clearances caused by rotor deformation and stator deformation.

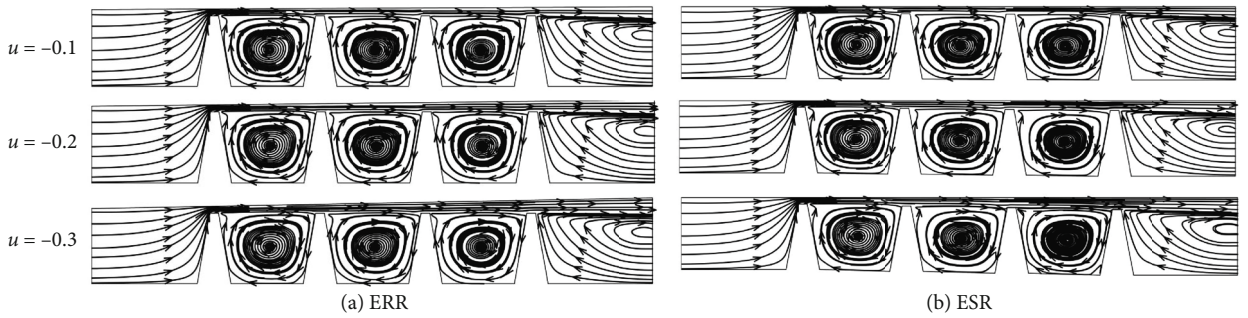

Figure 8: Flow structure in the labyrinth seal (Re = 10000, $\pi = 1.3$, $M_U = 0.23$, and $C = 0.067$).

distribution, the pressure coefficients of tooth cavities and pressure loads of labyrinth teeth are depicted in Figure 9. It is not surprising that the pressure coefficient decreases gradually along the flow direction due to the total pressure drop effect. However, the pressure load of labyrinth tooth present an opposite trend between the convergent type and the divergent type, in which the tooth pressure load of the convergent type grows up and that of the divergent type falls down from inlet to outlet. Nevertheless, the pressure coefficients of tooth cavities and pressure loads of labyrinth teeth are almost the same between the ESR and the ERR, proving again that the flow sensitivity of straight-through labyrinth seals to the clearance nonuniformity cause is very weak.

As one of most important quantity to describe leakage flow, the flow coefficient is also discussed including the ESR and the ERR. Figure 10 compares variations of flow coefficient with pressure ratio under different nonuniform clearances ($|u| = 0.1$, $|u| = 0.2$, and $|u| = 0.3$). From the results, when the minimum tip clearance is the same, characteristic lines of flow coefficient to pressure ratio gradually move upward with the increase of the absolute value of the nonuniformity coefficient, which indicates that under the same operating environment (constant circumferential Mach number, constant pressure ratio, and constant Reynolds number), the leakage flow increases with the rise of tip clearance nonuniformity. This is because except for the minimum tip clearance, the rest tip clearances increase with the rise of tip clearance nonuniformity, regardless of convergent type clearance or the divergent type clearance. When tip clearances of straight-through labyrinths become larger, the equivalent circulation area increases. At the same time, the kinetic energy carry-over factor also increases [6], resulting weaker total pressure dissipation in the tooth cavities. As for the effect of nonuniformity cause, when nonuniformity coefficient u is the same, there is no significant difference in the characteristics of flow coefficient to pressure ratio between the ESR and the ERR, regardless of the convergent type or the divergent type. For $|u| = 0.1$, $|u| = 0.2$, and $|u| = 0.3$, the maximum deviation between labyrinth seals with equal stator radius and equal rotor radius is less than 0.8%. Therefore, in the follow-up of this study, only the labyrinth seals with equal stator radius, as shown in Figure 2, are discussed about the influence of nonuniform tip clearance.

3.2. Effects of Nonuniformity Type

3.2.1. Subcritical State. The axial inertia of the airflow in the labyrinth seal can be reflected by the axial Mach number. Under typical subcritical state (Re = 10000, $\pi = 1.3$, $M_U = 0.23$, and $C = 0.067$), Figure 11 compares the axial Mach number distributions in the labyrinths with different clearance nonuniformity type (convergent type and divergent type). For labyrinths with convergent type clearance ($u > 0$), the axial Mach number increases gradually along the flow

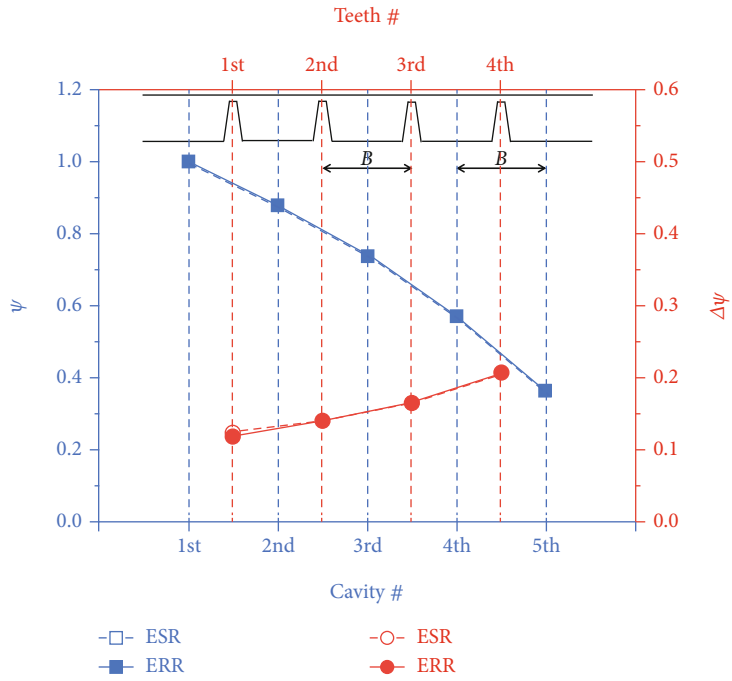

(a) $u = 0.1$

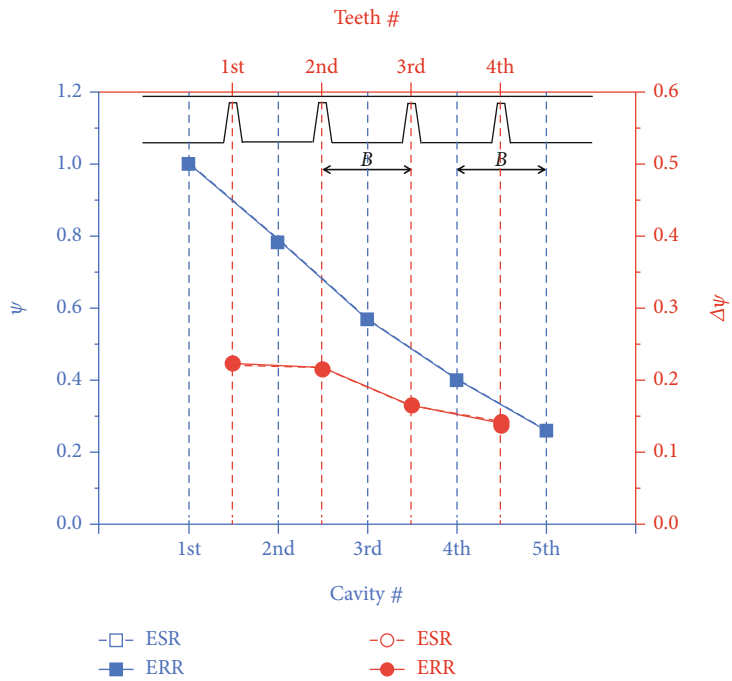

(b) $u = -0.1$

Figure 9: Continued.

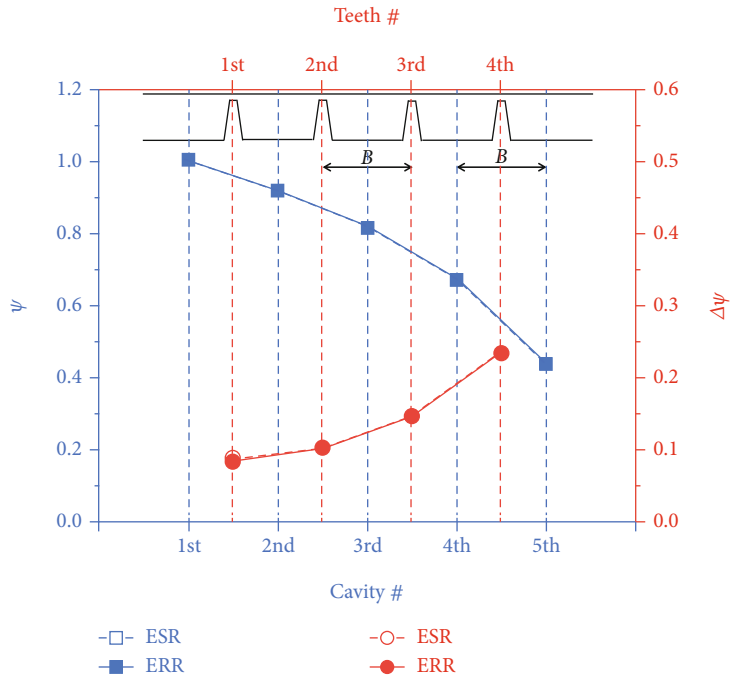

(c) $u = 0.2$

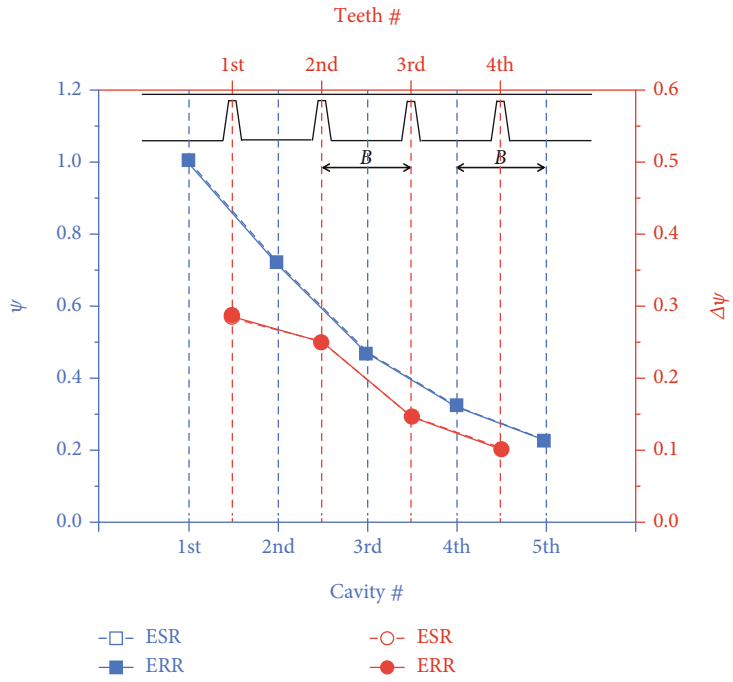

(d) $u = -0.2$

Figure 9: Continued.

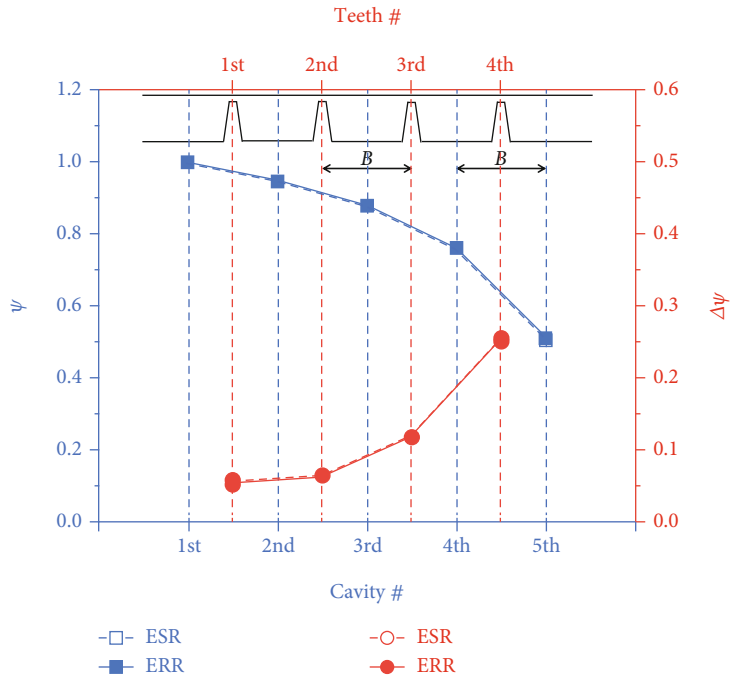

(e) $u = 0.3$

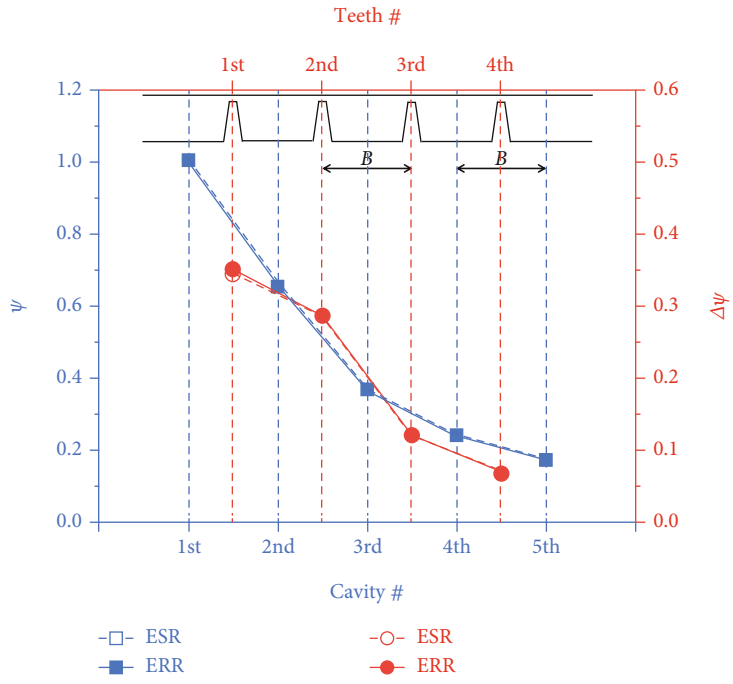

(f) $u = -0.3$

Figure 9: Pressure distributions of tooth cavities and pressure loads of labyrinth teeth (Re = 10000, $\pi = 1.3$, $M_U = 0.23$, and $C = 0.067$).

direction. The maximum axial Mach number appears at the last tip clearance. The axial Mach number at the front three tip clearance is small, and the axial inertia is weak, which is conducive to the dissipation from kinetic energy to thermal energy inside the tooth cavities. For labyrinths with divergent type clearance ($u < 0$), the axial Mach number decreases gradually along the flow direction. The maximum axial Mach number appears at the first tip clearance. The airflow with high axial velocity passes through the teeth cavity and directly to the next tip clearance. The kinetic energy carry-over effect of divergent type ($u < 0$) gets more significant than that of convergent type ($u > 0$). When $|u|$ is the same, the axial Mach number at the front three tip clearances of convergent type clearance labyrinths is generally smaller than that of divergent type clearance labyrinths. This shows that the airflow inside divergent type clearance labyrinth seals has greater axial inertia.

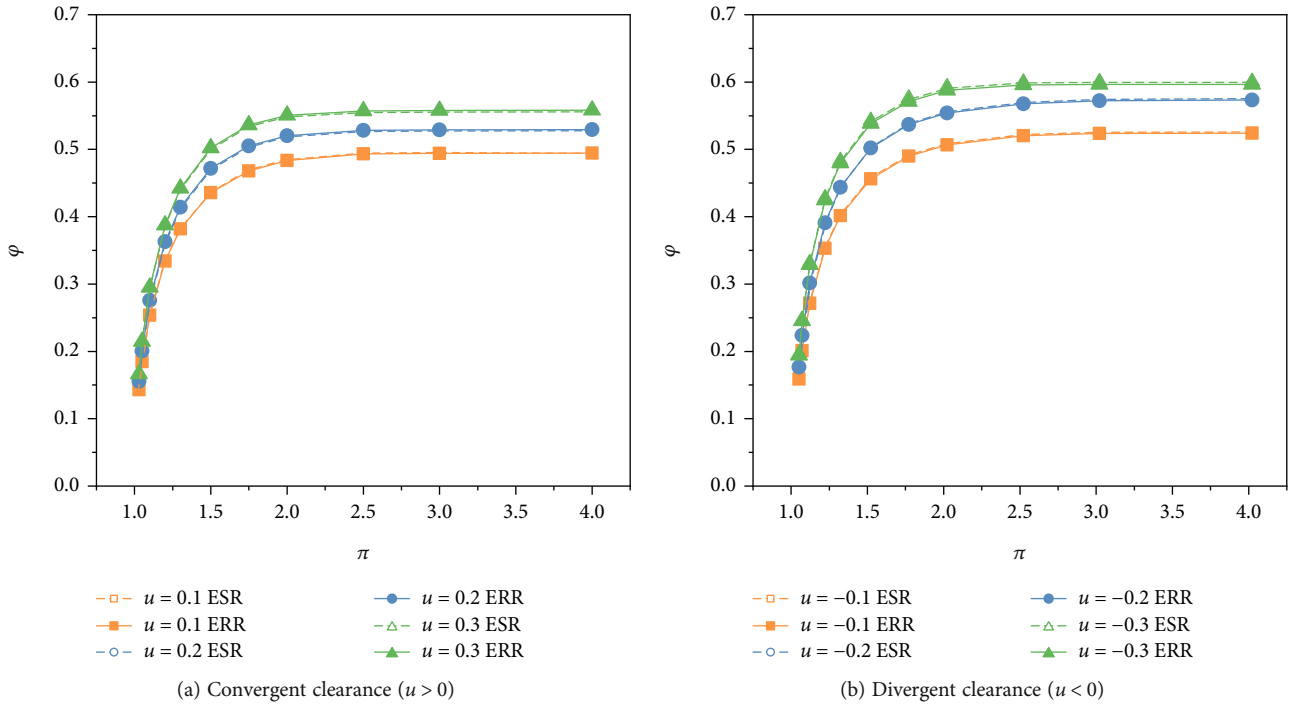

(a) Convergent clearance ($u > 0$)

(b) Divergent clearance ($u < 0$)

FIGURE 10: Variations of flow coefficient with pressure ratio under different nonuniform clearances (Re = 10000, $M_U = 0.23$, and $C = 0.067$).

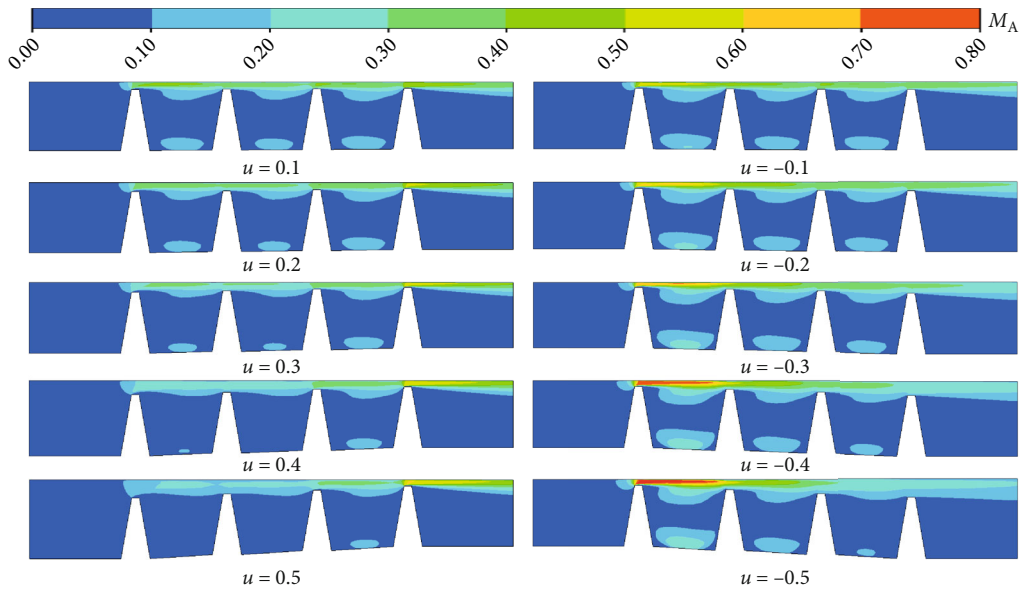

FIGURE 11: Axial Mach number distributions of nonuniform tip clearance labyrinths in the subcritical state (Re = 10000, $\pi = 1.3$, $M_U = 0.23$, and $C = 0.067$).

The pressure load of labyrinth tooth can also be influenced by the clearance nonuniformity significantly. Figure 12 compares the teeth pressure loads between the convergent type and the divergent type under different clearance nonuniformity degree ($-0.5 \le u \le 0.5$). For the labyrinths with uniform clearance ($u = 0$), the teeth pressure loads are almost uniform, which is approximately between 0.17 and 0.18. However, for the labyrinths with nonuniform clearance ($u \neq 0$), the teeth pressure loads of four stages also exhibit a nonuniform profile. It is remarkable that the teeth pressure load varies monotonously from the first stage to the fourth stage. But an obvious difference between the two nonuniformity types is that the teeth pressure load of convergent type ($u > 0$) increases monotonically, and the teeth pressure load of divergent type ($u < 0$) decreases monotonically along the flow direction. Comparing the convergent type and the divergent type, an interesting phenomenon is found that the teeth pressure load of third stage is all similar in cases of $|u| = 0.1$, $|u| = 0.2$, $|u| = 0.3$, $|u| = 0.4$, and $|u| = 0.5$ despite the opposite distribution trends. Moreover, the teeth

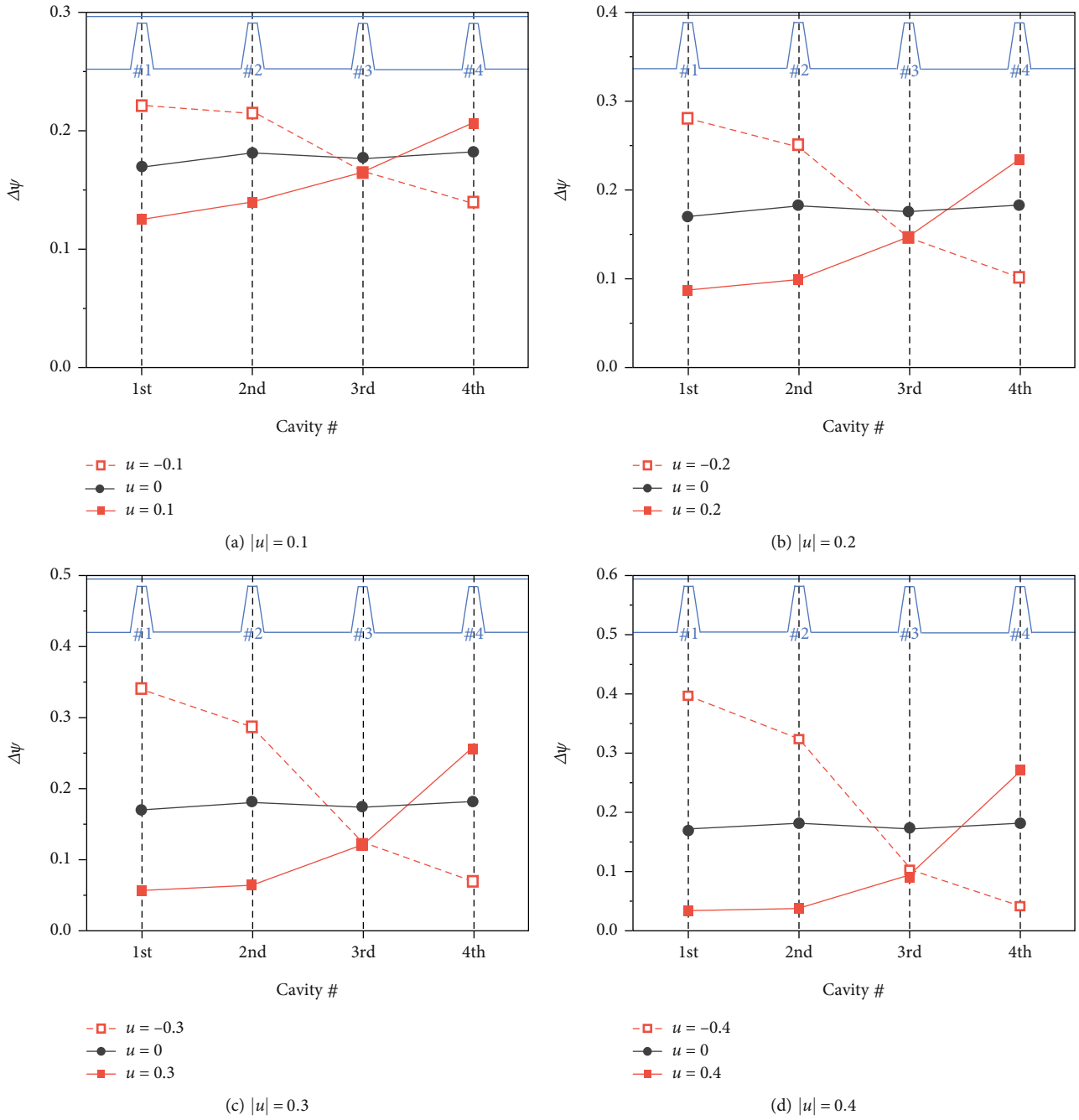

Figure 12: Continued.

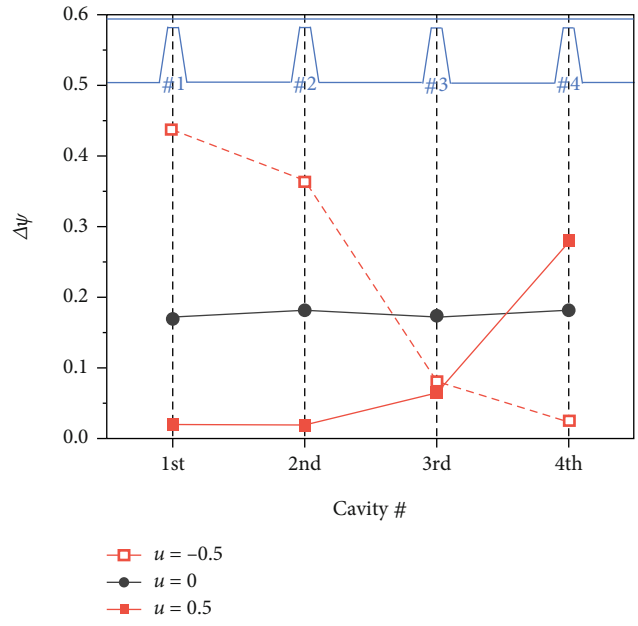

(e) $|u| = 0.5$

Figure 12: Teeth pressure loads in the subcritical state (Re = 10000, $\pi = 1.3$, $M_U = 0.23$, and $C = 0.067$).

Table 3: Maximum deviation of different teeth pressure loads in the subcritical state (Re = 10000, $\pi = 1.3$, $M_U = 0.23$, and $C = 0.067$).

$\lvert u\rvert$		0.1	0.2	0.3	0.4	0.5
$\lvert\Delta\psi_{max}-\Delta\psi_{min}\rvert$	$u > 0$	0.08	0.15	0.20	0.24	0.26
	$u < 0$	0.08	0.18	0.27	0.35	0.41

pressure load difference between the first stage and the last stage (maximum deviation) gradually rises with the increase of the clearance nonuniformity degree, that is, the absolute value of the nonuniformity coefficient $|u|$, as shown in Table 3. The results indicate that the maximum teeth pressure load deviation of the divergent type ($u < 0$) increases at a faster rate than that of the convergent type ($u > 0$). By contrast, the divergent nonuniformity type contributes more to the nonuniform teeth pressure load profile in the subcritical state.

3.2.2. Critical State. In the typical critical state (Re = 10000, $\pi = 4$, $M_U = 0.23$, $C = 0.067$, and $u = 0$), Figure 13 shows the axial Mach number distribution of a uniform tip clearance labyrinth. When the air flows through a labyrinth seal, due to the large total pressure loss, the total pressure of the last stage tip clearance is the lowest among all the stages. As mass flow rate is continuous, the axial velocity at the last stage tip clearance is the largest, so the last stage tip clearance enters the critical state first as shown in Figure 13.

Under the critical state (Re = 10000, $\pi = 4$, $M_U = 0.23$, and $C = 0.067$), the axial Mach number distributions in the labyrinths with different clearance nonuniformity type (convergent type and divergent type) are compared in Figure 14. For convergent type clearance labyrinths ($u > 0$), the critical section is the last stage tip clearance all the cases, so the maximum flow capacity of the labyrinth seal is limited by the last stage tip clearance. With the increase of nonuniformity coefficient, the axial Mach number at the front three tip clearances gradually reduces. For the divergent clearance labyrinth ($u < 0$), when the nonuniformity coefficient is small, such as the case of $u = -0.1$, the difference between the four tip clearances is not obvious. Although the area of the last stage tip clearance is the largest, it is still the first one to enter the critical state. As the clearance nonuniformity degree increases gradually, such as $u = -0.3$, $u = -0.4$, and $u = -0.5$, the critical section switches from the last stage tip clearance to the first stage tip clearance. The maximum flow capacity of the labyrinth seal is limited by the first stage tip clearance. Similar to the subcritical state, the kinetic energy carry-over effect of divergent type ($u < 0$) gets more significant than that of convergent type ($u > 0$).

In the critical state (Re = 10000, $\pi = 4$, $M_U = 0.23$, and $C = 0.067$), the teeth pressure loads under different clearance nonuniformity degree ($-0.5 \le u \le 0.5$) are also compared between the convergent type and the divergent type in Figure 15. Different from the subcritical state, the teeth pressure loads in the critical state is not uniform, even if the seal clearance is uniform ($u = 0$). The teeth pressure load of the last stage is significantly larger than those of the front three stages. For labyrinths with convergent type clearance ($u > 0$), the distributions of teeth pressure loads in the teeth cavities are similar to that of the labyrinth with uniform clearance ($u = 0$). Contrast to the uniform clearance labyrinth, the teeth pressure loads of the front three stages are lower, while that of the last stage is higher. For labyrinths with divergent type clearance ($u < 0$), the variation of the teeth pressure load is no longer monotonic along the flow direction. The largest teeth pressure load is still the last stage when the clearance nonuniformity is not obvious ($u = -0.1$), but with the increase

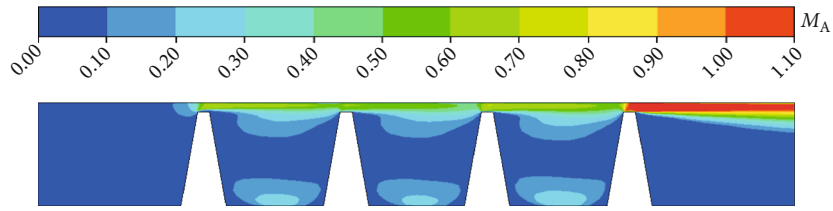

Figure 13: Axial Mach number distributions of uniform tip clearance labyrinth in the critical state (Re = 10000, $\pi = 4$, $M_U = 0.23$, $C = 0.067$, and $u = 0$).

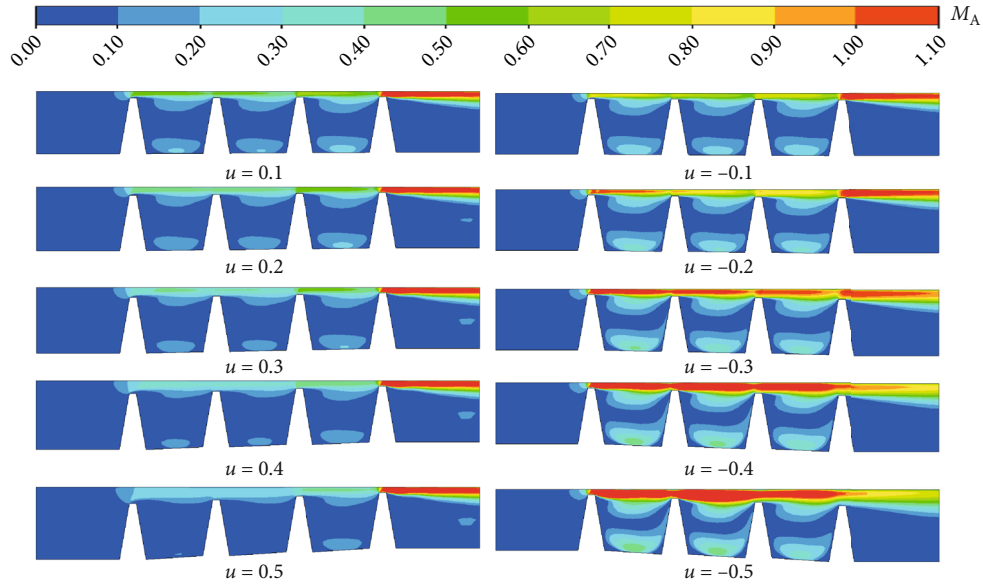

Figure 14: Axial Mach number distributions of nonuniform tip clearance labyrinths in the critical state (Re = 10000, $\pi = 4$, $M_U = 0.23$, and $C = 0.067$).

of the nonuniformity degree ($u = -0.2$, $u = -0.3$, $u = -0.4$, and $u = -0.5$), the distributions of teeth pressure loads in the teeth cavities become different from those of labyrinths with uniform clearance and convergent clearance. Although the first stage tip clearance is the critical section, the second stage develops into the key teeth for total pressure drop and undertakes the largest single teeth pressure load. Starting at the second stage, the teeth pressure load decreases monotonically along the flow direction. Similar to the subcritical state, the teeth pressure load maximum deviation gradually rises with the increase of the absolute value of the nonuniformity coefficient $|u|$, as shown in Table 4, meaning the clearance nonuniformity can promote the teeth pressure load deviation among the four stage. Opposed to the subcritical state, the maximum teeth pressure load deviation of the convergent type ($u > 0$) increases at a faster rate than that of the divergent type ($u < 0$). By contrast, the convergent nonuniformity type contributes more to the nonuniform teeth pressure load profile in the critical state.

3.3. Effects of Nonuniformity Degree

3.3.1. Pressure Coefficient. Due to nonuniform tip clearances, the law of kinetic energy dissipation will be different from that of uniform clearance labyrinths. The distribution of total pressure in the tooth cavities will also change with clearance nonuniformity degree. Figure 16 shows pressure coefficient distributions in the teeth cavities of subcritical state (Re = 10000, $\pi = 1.3$, $M_U = 0.23$, and $C = 0.067$) and critical state (Re = 10000, $\pi = 4$, $M_U = 0.23$, and $C = 0.067$), respectively. The pressure coefficient in the teeth cavities reduces gradually along the flow direction, bur the decrease tendency is not the same under different clearance nonuniformity coefficient. When aerodynamic boundary parameters and other geometric structure parameters are all the same, the pressure coefficients in the teeth cavities of the convergent type are higher than that of the divergent type with the equal clearance nonuniformity degree $|u|$. Compared with uniform clearance labyrinth seals, the difference of total pressure distributions may change the axial aerodynamic load of nonuniform clearance labyrinth seals.

Although the ratio of inlet total pressure to outlet static pressure is the same, pressure coefficients at the labyrinth outlet with different nonuniform coefficients are not the same. According to Figure 16, the outlet pressure coefficient of the convergent type clearance labyrinth gets larger with the increase of nonuniformity degree, meaning that the proportion of total pressure dissipation from inlet to outlet decreases. Situations for divergent type clearance labyrinths are just the opposite. Figure 17 shows the labyrinth seal

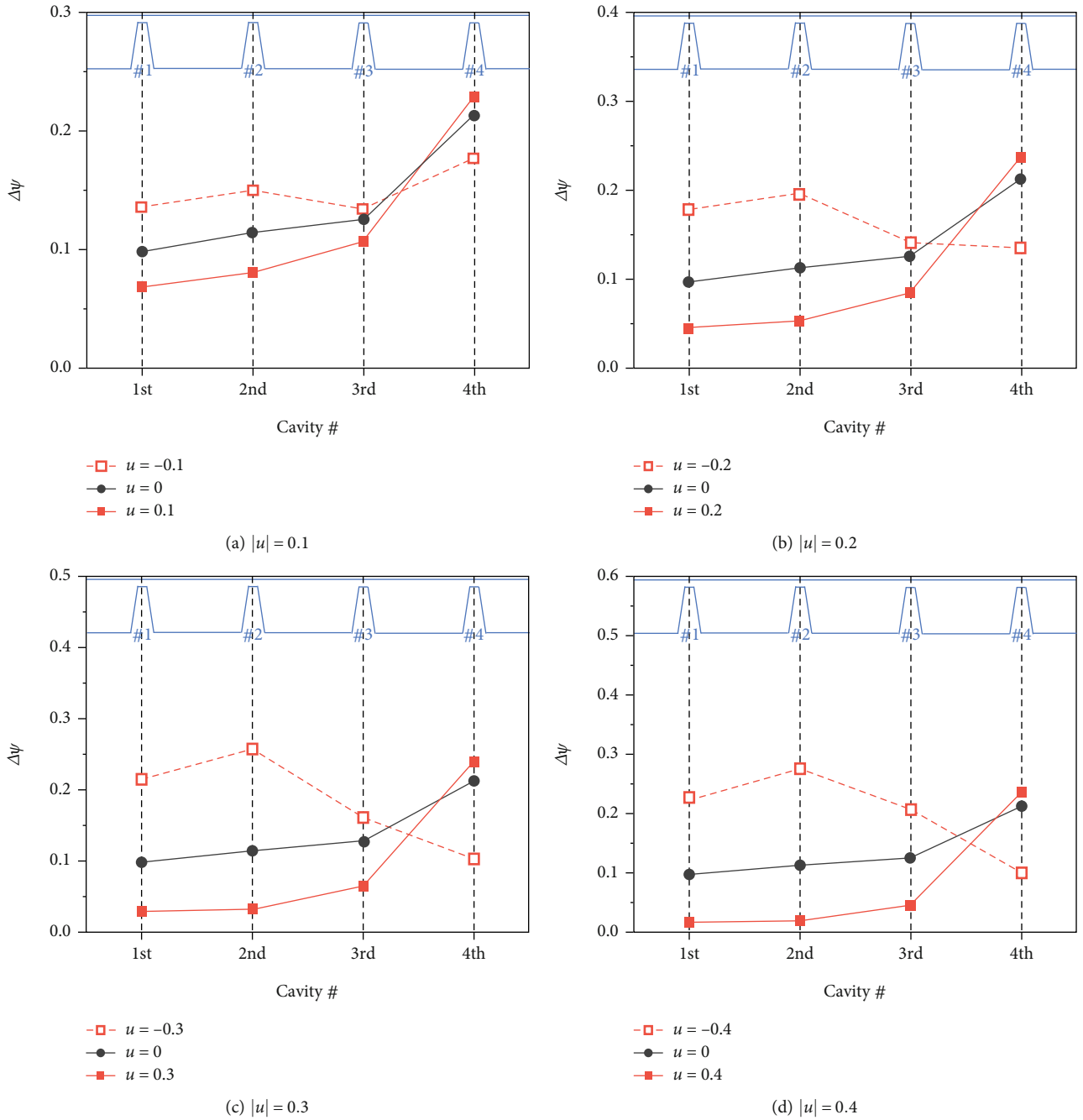

(a) $|u| = 0.1$

(b) $|u| = 0.2$

(c) $|u| = 0.3$

(d) $|u| = 0.4$

Figure 15: Continued.

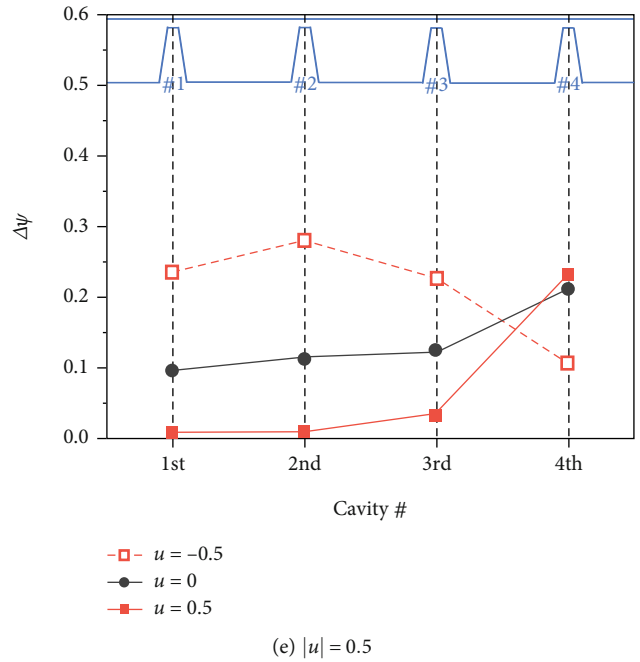

(e) $|u| = 0.5$

Figure 15: Teeth pressure loads in the critical state (Re = 10000, $\pi = 4$, $M_U = 0.23$, and $C = 0.067$).

Table 4: Maximum deviation of different teeth pressure loads in the critical state (Re = 10000, $\pi = 4$, $M_U = 0.23$, and $C = 0.067$).

$\lvert u\rvert$		0.1	0.2	0.3	0.4	0.5
$\lvert\Delta\psi_{max}-\Delta\psi_{min}\rvert$	$u > 0$	0.16	0.19	0.21	0.22	0.22
	$u < 0$	0. 04	0.06	0.15	0.18	0.18

pressure loads in the subcritical state (Re = 10000, $\pi = 1.3$, $M_U = 0.23$, and $C = 0.067$) and critical state (Re = 10000, $\pi = 4$, $M_U = 0.23$, and $C = 0.067$), respectively. With the increase of the absolute value of the nonuniformity coefficient |u|, seal pressure load of convergent type gradually falls down, while that of divergent type gradually grows up, regardless of subcritical state or critical state. The seal pressure load represents the ability to realize the total pressure drop, which is one of important aspect to evaluate the seal performance. In terms of total pressure drop, when the dimensionless minimum tip clearance is the same, convergent clearance contributes less to the total pressure drop with the increase of the clearance nonuniformity, while divergent clearance contributes more to the total pressure drop with the increase of the clearance nonuniformity.

3.3.2. Flow Coefficient. When the minimum tip clearance is the same, the average tip clearance of nonuniform clearance labyrinths is larger than that of uniform clearance labyrinths. Obviously, the labyrinth with smaller average tip clearance has stronger sealing ability if the minimum tip clearance is the same. Therefore, on the premise of the same minimum tip clearance, it is easy to infer that the labyrinth seals with nonuniform tip clearance have more leakage flow than that of the labyrinth seals with uniform tip clearance. Thereby, the nonuniformity impact factor is bound to be greater than 1. However, the growth rate of the leakage flow will be different under different nonuniformity degree. The variation of the nonuniformity impact factor with the clearance nonuniformity coefficient is analyzed to clarify the effect of clearance nonuniformity on the leakage flow.

Figures 18–21 show the variations of nonuniformity impact factor with nonuniformity coefficient under different Reynolds numbers, pressure ratios, circumferential Mach numbers, and dimensionless minimum tip clearances ($500 \le \mathrm{Re} \le 25000$, $1.03 \le \pi \le 4$, $0.23 \le M_U \le 0.92$, $0.033 \le C \le 0.100$, and $-0.5 \le u \le 0.5$), respectively. If minimum tip clearances are the same, two common points can be found. One is that when absolute values of nonuniformity coefficients are the same, nonuniformity impact factors of divergent type clearance labyrinths are larger than that of convergent type clearance labyrinths, meaning the seal performance of the convergent type is better than that of the divergent type. The other is that when clearance nonuniformity is small, characteristic lines of nonuniformity impact factor have little dispersion. Within the range of $-0.1 < u < 0.1$, under the same nonuniformity coefficient, deviations of nonuniformity impact factor under different operation conditions (Reynolds number, pressure ratio, circumferential Mach number, and dimensionless minimum tip clearance) are no more than 1.2%, which indicates that the effect of nonuniformity degree on the leakage flow is irrelevant to the operation conditions. In addition, other variation characteristics of the nonuniformity impact factor are also described in detail.

Variations of the nonuniformity impact factor at different Reynolds numbers ($500 \le \mathrm{Re} \le 25000$) are compared in Figure 18. Except for the cases of small Reynolds number (Re = 500 and Re = 1000), there is little deviation between variation curves of nonuniformity impact factor when

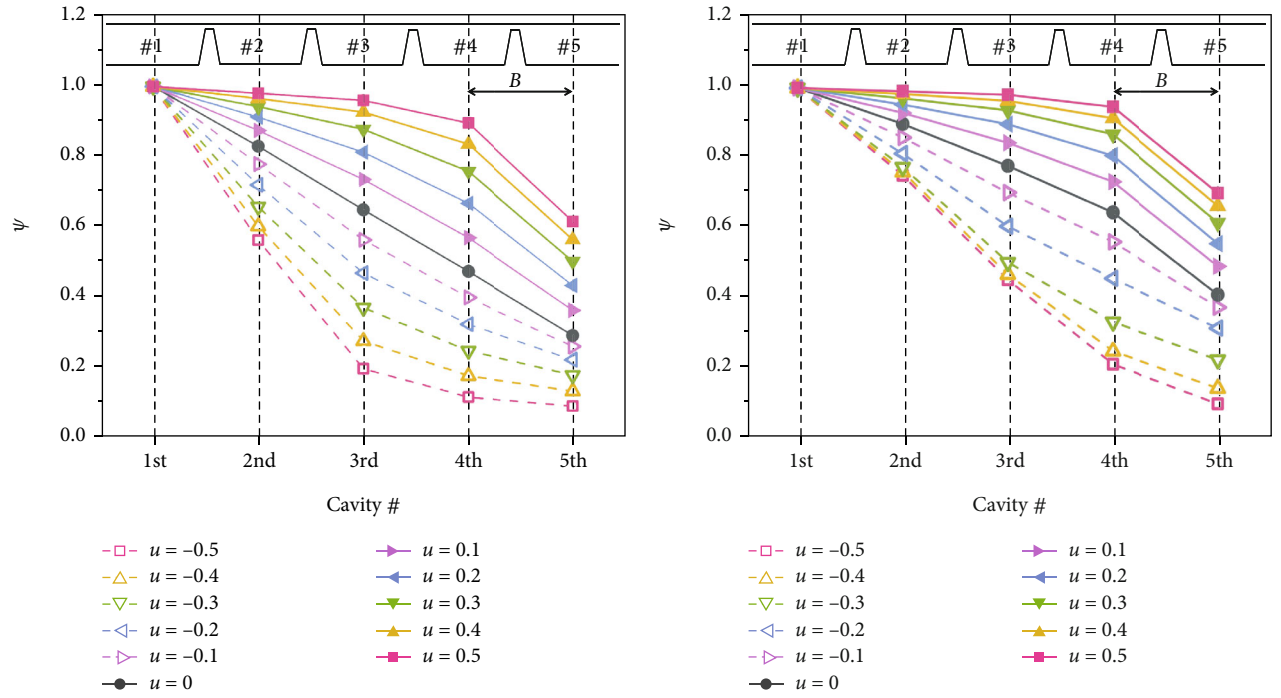

(a) Subcritical state (Re = 10000, $\pi = 1.3$, $M_U = 0.23$, and $C = 0.067$)

(b) Critical state (Re = 10000, $\pi = 4$, $M_U = 0.23$, and $C = 0.067$)

Figure 16: Total pressure distributions of different teeth cavities.

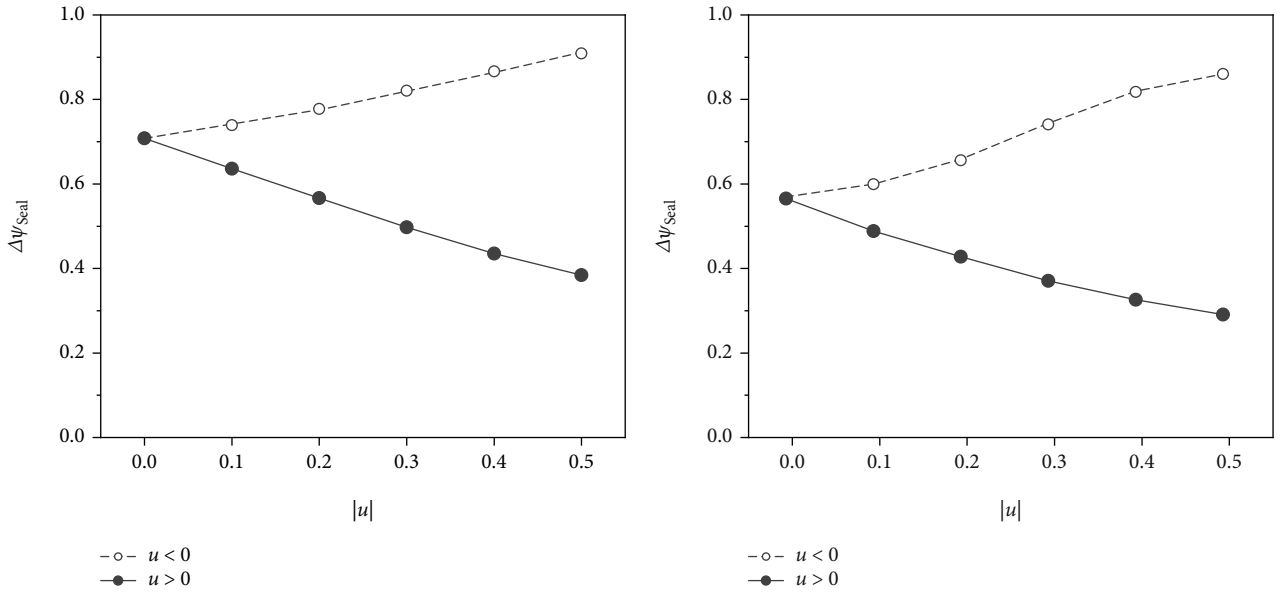

(a) Subcritical state (Re = 10000, $\pi = 1.3$, $M_U = 0.23$, and $C = 0.067$)

(b) Critical state (Re = 10000, $\pi = 4$, $M_U = 0.23$, and $C = 0.067$)

Figure 17: Labyrinth seal pressure loads.

Reynolds numbers are different. Under the actual operating conditions of aeroengines, the Reynolds number is usually much larger than 500 and 1000, so the influence of Reynolds number on the characteristic of nonuniformity impact factor to nonuniformity coefficient is not obvious. In the high Reynolds number range, the influence of Reynolds number can be ignored when analyzing the effect of clearance nonuniformity on the leakage flow.

Variations of nonuniformity impact factor at different pressure ratios ($1.03 \le \pi \le 4$) are compared in Figure 19. With the increase of pressure ratio, characteristic lines of nonuniformity impact factor gradually move down, meaning that the rise of leakage flow caused by nonuniform clearance is suppressed. When the sealing flow enters the critical state ($\pi = 2.5$, $\pi = 3$, and $\pi = 4$), pressure ratio has little influence on the variation curve of nonuniformity impact factor.

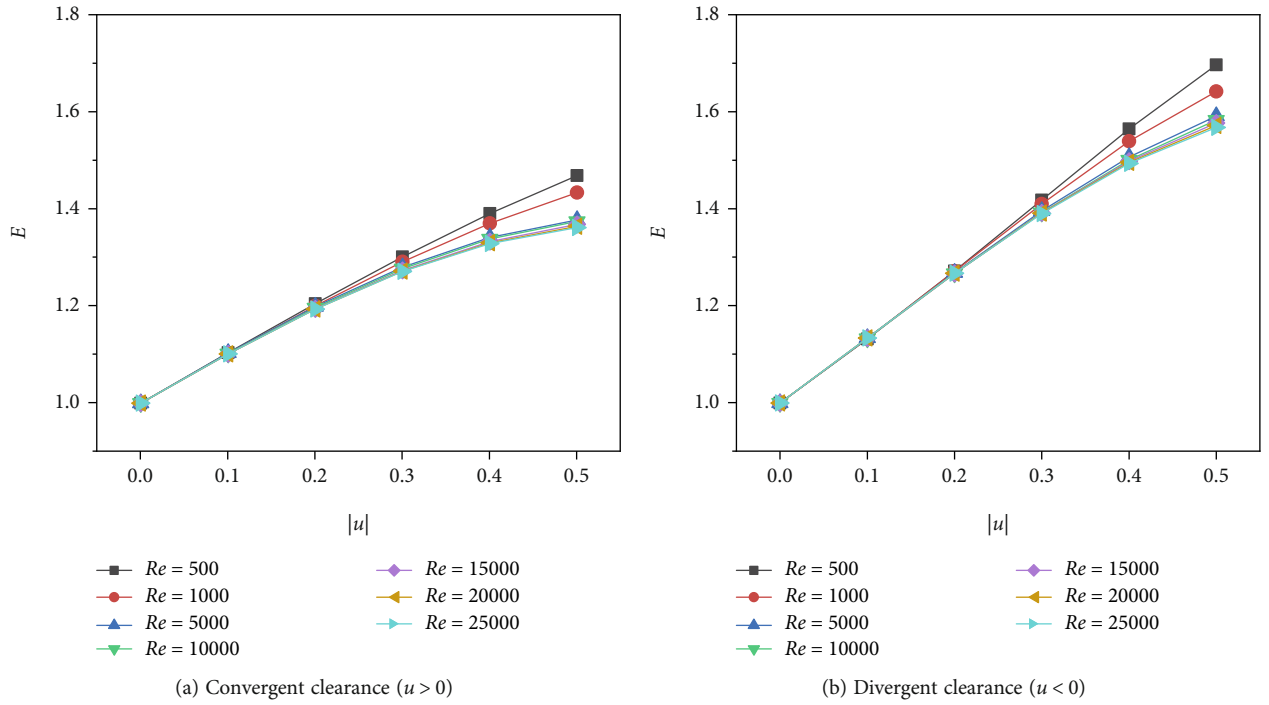

(a) Convergent clearance ($u > 0$) (b) Divergent clearance ($u < 0$)

Figure 18: Variations of nonuniformity impact factor under different Reynolds number ($\pi = 1.1$, $M_U = 0.23$, and $C = 0.067$).

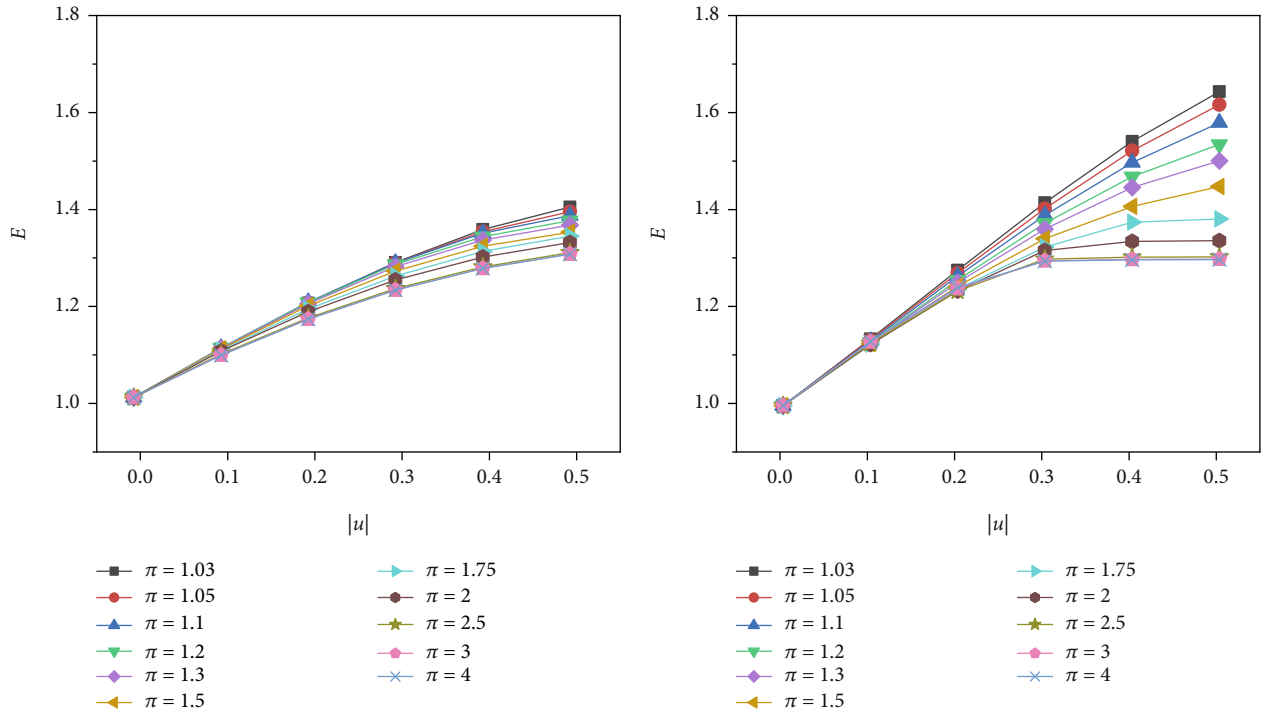

(a) Convergent clearance ($u > 0$) (b) Divergent clearance ($u < 0$)

Figure 19: Variations of nonuniformity impact factor under different pressure ratios (Re = 10000, $M_U = 0.23$, and $C = 0.067$).

Therefore, the leakage flow of labyrinths in the subcritical state (small pressure ratio) will be affected more significantly by the nonuniform clearance. And the influence of pressure ratio can be ignored when the seal flow enters the critical state (large pressure ratio).

Variations of nonuniformity impact factor at different circumferential Mach numbers ($0.23 \le M_U \le 0.92$) are compared in Figure 20. With the increase of circumferential Mach number, the characteristic lines of nonuniformity impact factor gradually move up, meaning that the rise of

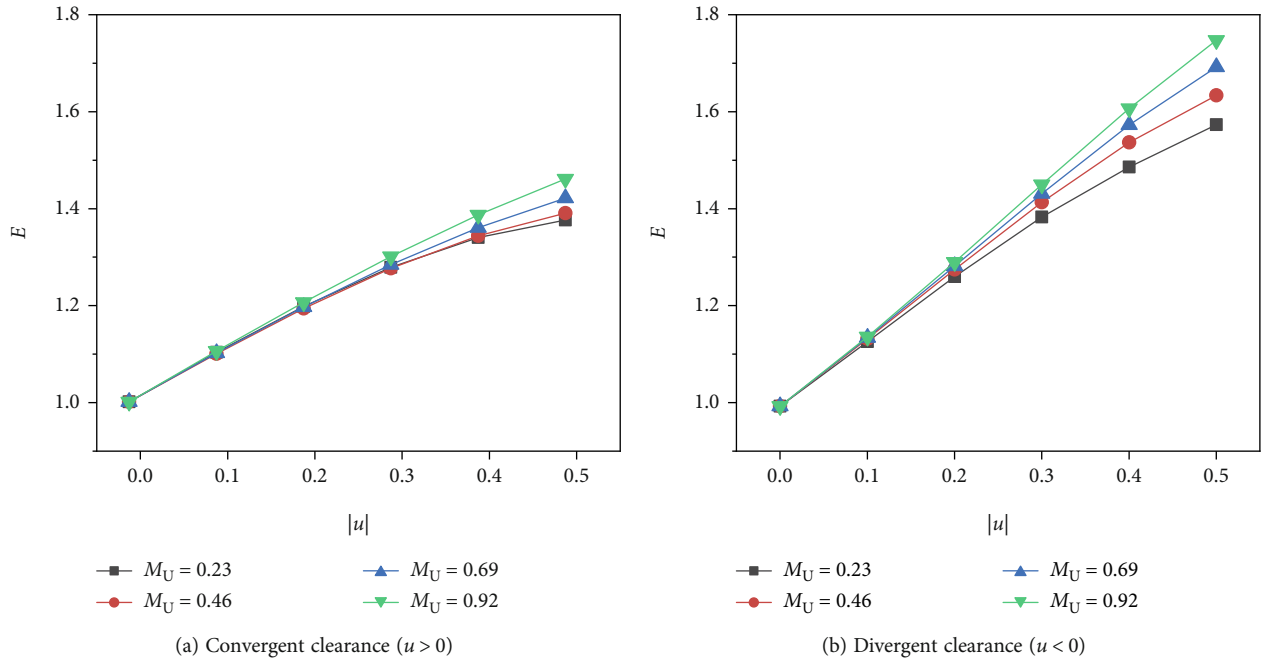

(a) Convergent clearance ($u > 0$)

(b) Divergent clearance ($u < 0$)

Figure 20: Variations of nonuniformity impact factor under different circumferential Mach numbers (Re = 10000, $\pi = 1.1$, and $C = 0.067$).

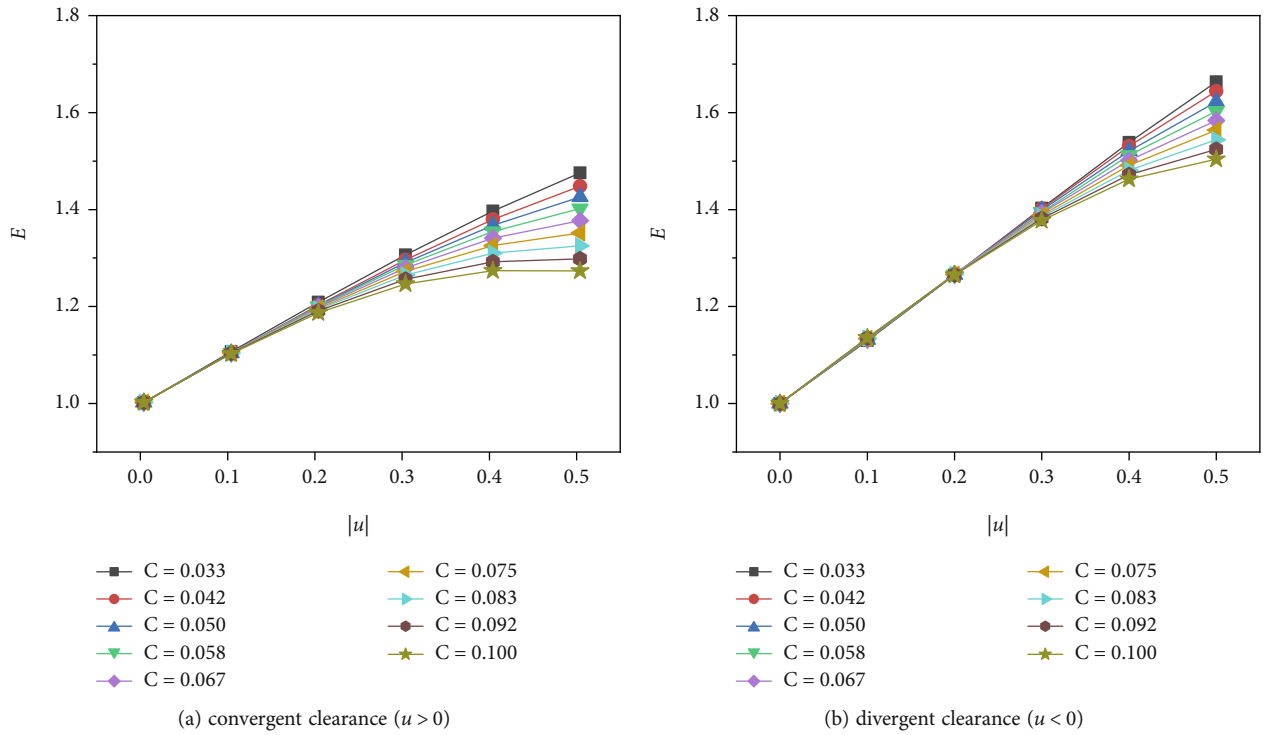

(a) convergent clearance ($u > 0$)

(b) divergent clearance ($u < 0$)

Figure 21: Variations of nonuniformity impact factor under different dimensionless minimum tip clearances (Re = 10000, $\pi = 1.1$, $M_U = 0.23$).

leakage flow caused by nonuniform clearance is aggravated. The results indicate that the labyrinth seal located at high radius location in the aeroengines will be affected more obviously by the clearance nonuniformity. Meanwhile, when the aeroengines operate at high speed, the leakage flow of labyrinth will be also affected more significantly by the nonuniform clearance. Because the higher radius and the higher rotating speed contribute the larger circumferential Mach numbers.

Variations of nonuniformity impact factor at different dimensionless minimum tip clearances ($0.033 \le C \le 0.100$) are compared in Figure 21. With the increase of dimensionless

minimum tip clearance, the characteristic lines of nonuniformity impact factor gradually move down, meaning that the rise of leakage flow caused by nonuniform clearance is suppressed. For labyrinth seals with the same tooth pitch in aeroengines, the leakage flow of labyrinth seals clearance with smaller sealing clearance will be affected more significantly by the nonuniform clearance.

4. Conclusions

In this work, nonuniform clearance effects on pressure distribution and leakage flow in straight-through labyrinths are investigated by numerical simulation, including nonuniformity cause (rotor deformation or stator deformation), nonuniformity type (convergent clearance or divergent clearance), and no-uniformity degree (nonuniformity coefficient). The pressure coefficient and the flow coefficient of labyrinth seals with equal stator radius (ESR) and equal rotor radius (ERR) is compared to clarify the effect of nonuniformity cause. Distributions of axial Mach number and pressure load are discussed for convergent and divergent type clearance labyrinths to analyze the effect of nonuniformity type. The variations of nonuniformity impact factor are also studied under different Reynolds numbers, pressure ratios, circumferential Mach numbers, and dimensionless minimum tip clearances to visualize the effect of nonuniformity degree. This paper draws the following conclusions:

(i) For typical nonuniform clearance labyrinths in aeroengines ($u = \pm 0.1$, ± 0.2, and ± 0.3), there is no significant influence of nonuniformity cause (rotor deformation or stator deformation) on the pressure coefficient and the flow coefficient. The maximum flow coefficient deviation between the ESR and the ERR is less than 0.8%

(ii) When absolute values of nonuniformity coefficients are the same, nonuniformity impact factors of divergent type clearance labyrinths are larger than that of convergent type clearance labyrinths, meaning the seal performance of the convergent type is better than that of the divergent type

(iii) When the absolute value of the nonuniformity coefficient $|u|$ is less than 0.1, the effect of the nonuniformity degree on the leakage flow is almost irrelevant to the operating conditions. In the parameter range of the current study, deviations of nonuniformity impact factor under different operating conditions (Reynolds number, pressure ratio, circumferential Mach number, and dimensionless minimum tip clearance) are no more than 1.2%.

(iv) Under the typical labyrinths operation range in aeroengines ($500 \le \mathrm{Re} \le 25000$, $1.03 \le \pi \le 4$, $0.23 \le M_U \le 0.92$, and $0.033 \le C \le 0.100$ and $-0.5 \le u \le 0.5$), compared with the uniform sealing clearance labyrinth with the same minimum tip clearance, the nonuniform labyrinth has a larger leakage flow. The effect of the nonuniform clearance is more obvious at small pressure ratio, high circumferential Mach number, and small dimensionless minimum tip clearance

Nomenclature

a: Local sound speed (m/s)
A: Cross-section area of the labyrinth tip clearance (m^2)
$A_{\min}$: Cross-section area of the labyrinth minimum tip clearance (m^2)
B: Labyrinth pitch (m)
c: Tip clearance of labyrinth (m)
C: Dimensionless minimum tip clearance
c_{av}: Average labyrinth tip clearance (m)
c_i: Labyrinth tip clearance of the i^{th} stage ($i = 1, 2, 3, 4$) (m)
$c_{\max}$: Maximum labyrinth tip clearance (m)
$c_{\min}$: Minimum labyrinth tip clearance (m)
E: Nonuniformity impact factor
H: Labyrinth tooth height (m)
L_i: Length of labyrinth inlet (m)
L_o: Length of labyrinth outlet (m)
M_A: Axial Mach number
M_U: Circumferential Mach number
$\dot{m}$: Leakage mass flow rate (kg/s)
$p_{s,\mathrm{out}}$: Static pressure of labyrinth outlet (Pa)
p_t: Total pressure (Pa)
$p_{t,\mathrm{in}}$: Total pressure of labyrinth inlet (Pa)
r: Radius of the labyrinth teeth tip (m)
R: Gas constant (J/(kg·K))
Re: Reynolds number
Re_ω: Rotational Reynolds number
t: Labyrinth tip width (m)
$T_{t,\mathrm{in}}$: Total temperature of seal inlet (K)
u: Clearance nonuniformity coefficient
V_{A}: Axial velocity (m/s)
V_θ: Tangential velocity (m/s)
α: inclination angle (degree)
φ: Flow coefficient
φ_u: Flow coefficient of the nonuniform clearance labyrinth
φ_0: Flow coefficient of the uniform clearance labyrinth
μ: Dynamic viscosity of labyrinth inlet (Pa·s)
ψ: Pressure coefficient
ψ_i: Pressure coefficient in the i^{th} teeth cavity ($i = 1, 2, 3, 4, 5$)
ψ_{inlet}: Pressure coefficient of labyrinth inlet
ψ_{outlet}: Pressure coefficient of labyrinth outlet
$\Delta\psi_{\mathrm{seal}}$: Pressure load of labyrinth seal
π: Ratio of inlet total pressure to outlet static pressure
ρ: Density of labyrinth inlet (kg/m^3)
Ω: Rotating speed (rad/s)

Data Availability

The data used to support the findings of this study are included within the article.

Conflicts of Interest

The authors declare that they have no conflicts of interest.

Acknowledgments

The authors gratefully acknowledge the fund from the National Science and Technology Major Project of China (Grant No. J2019-III-0003-0046) and the Special Research Project of Chinese Civil Aircraft (Grant No. MJ-2018-D-21).

References

[1] T. Nikolaidis, H. Wang, and P. Laskaridis, "Transient modelling and simulation of gas turbine secondary air system," *Applied Thermal Engineering*, vol. 170, article 115038, 2020.

[2] G. Liu, X. Kong, Y. Liu, and Q. Feng, "Effects of rotational speed on the leakage behaviour, temperature increase, and swirl development of labyrinth seal in a compressor stator well," *Proceedings of the Institution of Mechanical Engineers, Part G: Journal of Aerospace Engineering*, vol. 231, no. 13, pp. 2362–2374, 2017.

[3] K. C. Nayak, "Effect of rotation on leakage and windage heating in labyrinth seals with honeycomb lands," *Journal of Engineering for Gas Turbines and Power*, vol. 142, no. 8, article 081001, 2020.

[4] Z. Li, J. Li, X. Yan, and Z. Feng, "Effects of pressure ratio and rotational speed on leakage flow and cavity pressure in the staggered labyrinth seal," *Journal of Engineering for Gas Turbines and Power*, vol. 133, no. 11, article 114503, 2011.

[5] D. Hu, L. Jia, and L. Yang, "Dimensional analysis on resistance characteristics of labyrinth seals," *Journal of Thermal Science*, vol. 23, no. 6, pp. 516–522, 2014.

[6] T. Wu and L. S. Andrés, "Gas labyrinth seals: improved prediction of leakage in gas labyrinth seals using an updated kinetic energy carry-over coefficient," *Journal of Engineering for Gas Turbines and Power*, vol. 142, no. 12, article 121012, 2020.

[7] H. Qin, D. Lu, D. Zhong, Y. Wang, and Y. Song, "Experimental and numerical investigation for the geometrical parameters effect on the labyrinth-seal flow characteristics of fast reactor fuel assembly," *Annals of Nuclear Energy*, vol. 135, article 106964, 2020.

[8] A. Szymański, W. Wróblewski, K. Bochon, M. Majkut, M. Strozik, and K. Marugi, "Experimental validation of optimised straight-through labyrinth seals with various land structures," *International Journal of Heat and Mass Transfer*, vol. 158, article 119930, 2020.

[9] S. Subramanian, A. S. Sekhar, and B. V. S. S. S. Prasad, "Influence of combined radial location and growth on the leakage performance of a rotating labyrinth gas turbine seal," *Journal of Mechanical Science and Technology*, vol. 29, no. 6, pp. 2535–2545, 2015.

[10] Y. Zhao and C. Wang, "Shape optimization of labyrinth seals to improve sealing performance," *Aerospace*, vol. 8, no. 4, p. 92, 2021.

[11] T. Wu and L. S. Andrés, "Gas labyrinth seals: on the effect of clearance and operating conditions on wall friction factors - a CFD investigation," *Tribology International*, vol. 131, pp. 363–376, 2019.

[12] X. Yan, X. Dai, K. Zhang, J. Li, and K. He, "Effect of teeth bending and mushrooming damages on leakage performance of a labyrinth seal," *Journal of Mechanical Science and Technology*, vol. 32, no. 10, pp. 4697–4709, 2018.

[13] L. S. Andrés, J. Yang, and R. Kawashita, "On the effect of clearance on the leakage and cavity pressures in an interlocking labyrinth seal operating with and without swirl brakes: experiments and predictions," *Journal of Engineering for Gas Turbines and Power*, vol. 143, no. 3, article 031003, 2021.

[14] S. I. Lee, Y. J. Kang, W. J. Kim et al., "Effects of tip clearance, number of teeth, and tooth front angle on the sealing performance of straight and stepped labyrinth seals," *Journal of Mechanical Science and Technology*, vol. 35, no. 4, pp. 1539–1547, 2021.

[15] G. Li, Q. Zhang, E. Huang, Z. Lei, H. Wu, and G. Xu, "Leakage performance of floating ring seal in cold/hot state for aeroengine," *Chinese Journal of Aeronautics*, vol. 32, no. 9, pp. 2085–2094, 2019.

[16] X. Kong, G. Liu, Y. Liu, Z. Lei, and L. Zheng, "Performance evaluation of the inter-stage labyrinth seal for different tooth positions in an axial compressor," *Proceedings of the Institution of Mechanical Engineers, Part A: Journal of Power and Energy*, vol. 232, no. 6, pp. 579–592, 2018.

[17] X. Kong, G. Liu, Y. Liu, and L. Zheng, "Experimental testing for the influences of rotation and tip clearance on the labyrinth seal in a compressor stator well," *Aerospace Science and Technology*, vol. 71, pp. 556–567, 2017.

[18] D. Eastwood, D. D. Coren, C. A. Long et al., "Experimental investigation of turbine stator well rim seal, re-ingestion and interstage seal flows using gas concentration techniques and displacement measurements," *Journal of Engineering for Gas Turbines and Power*, vol. 134, no. 8, article 082501, 2012.

[19] V. Ganine, J. W. Chew, N. J. Hills, S. N. Mohamed, and M. M. Miller, "Transient aero-thermo-mechanical multidimensional analysis of a high pressure turbine assembly through a square cycle," *Journal of Engineering for Gas Turbines and Power*, vol. 143, no. 8, article 081008, 2021.

[20] F. Cangiolia, S. Chatterton, P. Pennacchi, L. Nettis, and L. Ciuchicchi, "Thermo-elasto bulk-flow model for labyrinth seals in steam turbines," *Tribology International*, vol. 119, pp. 359–371, 2018.

[21] D. Sun, S. Y. Li, H. Zhao, and C. W. Fei, "Numerical investigation on static and rotor-dynamic characteristics of convergent-tapered and divergent-tapered hole-pattern gas damper seals," *Materials*, vol. 12, no. 14, p. 2324, 2019.

[22] Y. Shi, S. Ding, T. Qiu, P. Liu, and C. Liu, "Nonuniform clearance effects on windage heating and swirl development in straight-through labyrinth seals," *Journal of Aerospace Engineering*, vol. 35, no. 3, article 04022016, 2022.

[23] G. Vannini, C. Mazzali, and H. Underbakke, "Rotordynamic computational and experimental characterization of a convergent honeycomb seal tested with negative preswirl, high pressure with static eccentricity and angular misalignment," *Journal of Engineering for Gas Turbines and Power*, vol. 139, no. 5, article 052502, 2017.

[24] A. J. M. Gamal and J. M. Vance, "Labyrinth seal leakage tests: tooth profile, tooth thickness, and eccentricity effects," *Journal of Engineering for Gas Turbines and Power*, vol. 130, no. 1, article 012510, 2008.

[25] U. Yucel and J. Y. Kazakia, "Analytical prediction techniques for axisymmetric flow in gas labyrinth seals," *Journal of Engineering for Gas Turbines and Power*, vol. 123, no. 1, pp. 255–257, 2001.

[26] J. Denecke, J. Färber, K. Dullenkopf, and H. J. Bauer, "Dimensional analysis and scaling of rotating seals," in *Proceedings of ASME Turbo Expo 2005: Power for Land, Sea and Air*, pp. 1149–1160, Reno, Nevada, USA, June 2005.

[27] J. A. Millward and M. F. Edwards, "Windage heating of air passing through labyrinth seals," *Journal of Turbomachinery*, vol. 118, no. 2, pp. 414–419, 1996.